12th Scientific/Research Symposium with International Participation
„METALLIC AND NONMETALLIC MATERIALS“ B&H, 19th-20th April 2018

PHASE EQUILIBRIA OF THE Cu-In-Ni TERNARY SYSTEM AT 300 °C

Aleksandar Đorđević[1], Milena Premović[1], Duško Minić[1], Vladan Ćosović[2], Milutin Živković[3], Ljubiša Balanović[4], Dragan Manasijević[4], Milan Kolarević[5]

[1]University in Priština, Faculty of Technical Science
K.M. 7, 4000 Kos. Mitrovica
Serbia
[2]University of Belgrade, Institute of Chemistry, Technology and Metallurgy
Njegoševa 12, 11000 Belgrade
Serbia
[3]Technical College of Mechanical Engineering Professional Studies
Radoja Krstića 19, 37240 Trstenik,
Serbia
[4]University of Belgrade, Technical Faculty in Bor
VJ 12, Bor
Serbia
[5]University of Kragujevac, Faculty of Mechanical and Civil Engineering
Dositejeva 19, 36000 Kraljevo
Serbia

Keywords: The Cu-In-Ni ternary system, isothermal section at 300 ºC, microstructural analysis

ABSTRACT

This study reports experimental and thermodynamic investigation of the Cu-In-Ni ternary system at 300 °C. Isothermal section of the Cu-In-Ni system at 300 °C was calculated using optimized thermodynamic parameters for the constitutive binary systems from literature. Microstructure analysis of selected alloy samples after long time annealing at 300 °C was carried out using scanning electron microscopy coupled with energy dispersive spectrometry (SEM-EDS) and X-ray powder diffraction (XRD) technique. Good agreement between thermodynamic calculations and experimental results was observed.

1. INTRODUCTION

Nickel and nickel-based alloys are widely used in different industries such as chemical, automotive, marine etc., for making vessels, pipes, heat exchangers, pumps, impellers, valves, and other type of equipment [1]. Furthermore, nickel with copper forms high-quality alloys with a variety of applications [2-11]. The most commonly used Ni-Cu alloy is Monel [12-14], which is primarily composed of nickel (up to 67%) and copper, with small amounts of iron, manganese, carbon, and silicon.

It is recognized that copper is a widely used material because of its high electrical and thermal conductivity. By adding a nickel to copper, it is possible to improve the mechanical properties and corrosion resistance of copper, while adding indium lowers its melting point.

To the extent of our knowledge, up to now, ternary Cu-In-Ni alloys have not been investigated from the point of view of mechanical and electrical properties. Furthermore, it can be expected that some of these ternary alloys may be excellent candidates for some of the aforementioned applications.
The Cu-In-Ni ternary system has been previously experimentally and thermodynamically assessed by Minic et al. [15]. In their study, Minic et al. [15] reported the liquidus surface, three vertical sections and isothermal sections at 400 ºC and 500 ºC.
In the current study phase diagram of the Cu-In-Ni ternary system 300 ºC is evaluated. Using SEM-EDS and XRD analyses are presented as well. The applied research procedure is similar to that given in [16-18] and it is aimed at providing better insight into properties of alloys which should contribute to further expansion of their application possibilities.

2. EXPERIMENTAL PROCEDURE

Nineteen ternary and three binary alloy samples (marked as a B1, B2, and B3) were prepared from copper, indium, and nickel (99.999 at. %) from Alfa Aesar (Germany) in an induction furnace under high-purity argon atmosphere. In general, the average mass loss during melting of samples was about 2 mass%. Alloy samples were placed in evacuated quartz tubes and sealed. Then alloy samples were annealed at 300 ºC for 4 weeks at high-temperature furnace (GSL1700X, Hefei Kejing Materials Technology Co., Ltd., Hefei, China) with estimated error of the temperature ±1 ºC. After annealing samples were quenched into a water and ice mixture in order to retain reached phase equilibrium. Annealed samples were cut into two parts. One part of the sample was subjected to microstructure analysis. It was prepared by the conventional metallographic procedure without etching. Polished side of the sample was first subjected to EDS elemental mapping to check compositional homogeneity and possible segregation. Further, overall compositions and compositions of coexisting phases were determined using EDS point and area analysis. Microstructure analysis was carried out on TESCAN VEGA3 scanning electron microscope with energy dispersive spectroscopy (EDS) (Oxford Instruments X-act).
The second part of the sample was grinded and examined using X-ray diffraction. XRD patterns of the studied samples were recorded on a D2 PHASER powder diffractometer equipped with a dynamic scintillation detector and ceramic X-ray Cu tube (KFLCu-2K) in a 2θ range of 5 to 75 deg with a step size of 0.02 deg. The patterns were analyzed using Topas 4.2 software and ICDD databases PDF2(2013).

3. RESULTS AND DISCUSSION

The isothermal section of the Cu-In-Ni ternary system at 300 ºC has been thermodynamically predicted using the optimized thermodynamic parameters for the constitutive binary systems from literature [19-21]. The parameters for the binary Cu–In a system were taken from Liu et al. [19], for the In–Ni system from Waldner and Ipser [20], and for the Cu–Ni binary system from Mey [21]. Calculations were performed using PANDAT software [22].
The list of phases from constitutive binary subsystems considered for thermodynamic binary-based prediction together with their corresponding Pearson symbols is given in Table 1.

Table 1. Considered phases in the Cu-In-Ni ternary system and their crystal structures

Phase name	Common name	Structure designation	Pearson symbol
LIQUID	Liquid	-	-
TETRAG_A6	(In)	*A*6	*tI*2
FCC_A1	(Cu,Ni)	*A*1	*cF*4
BCC_A2	β(Cu_4In)	*A2*	*cI*2
CUIN_DELTA	δ(Cu_7In_3)	. . .	*aP40*
CUIN_ETAP	η(Cu_2In)	$B8_2$	*hP*6
CUIN_ETA	η′(CuIn)	$B8_1$	*hP4*
CUIN_THETA	$Cu_{11}In_9$	…	*mC*20
CUIN_GAMMA	γ(Cu_9In_4)	. . .	*cP52*
NI3IN7	$Ni_{28}In_{72}$	...	*cI*40
NI2IN3	Ni_2In_3	$D5_{13}$	*hP5*
INNI_DELTA	δ(NiIn)	*B*2	*cP2*
NIIN	ε`(NiIn)	*B*35	*hP*6
INNI_CHI_PRIME	ζ`($Ni_{13}In_9$)	…	*mC*44
INNI_CHI	ζ	…	…
NI2IN	Ni_2In	$B8_2$	*hP6*
NI3IN	Ni_3In	$D0_{19}$	*hP*6

The calculated isothermal section of the Cu-In-Ni ternary system at 300 ºC is presented in Fig. 1. The alloy samples selected for experimental investigation are also marked in Fig. 1.

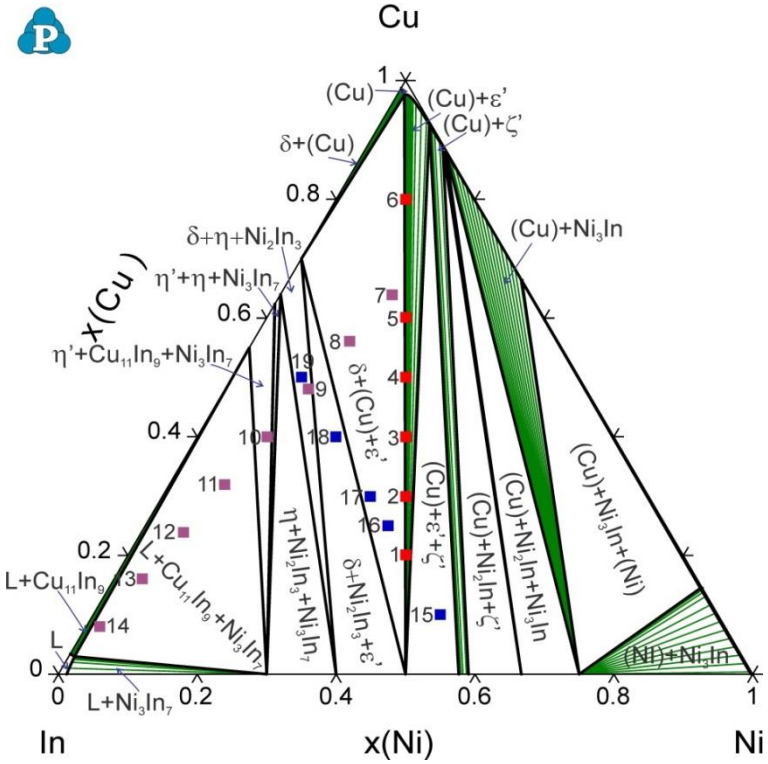

Fig. 1. Predicted isothermal section of the ternary Cu–In–Ni system at 300 °C with marked compositions of the studied samples

Compositions of the selected alloy samples stretch out along three vertical sections: Cu–In0.5Ni0.5, In-Cu0.8Ni0.2 and x(In) = 0.4 of the studied ternary system. All selected samples marked in Fig. 1 were investigated using the same experimental techniques. Seven phase regions were experimentally investigated. Six of the investigated regions were three-phase regions and the remaining one was a two-phase region.

The experimental results of EDS and XRD analyses are presented in Table 2.

Table 2. Experimentally determined phase compositions and lattice parameters of phases in the ternary Cu–In–Ni system at 300 °C

S.	Exp. phases	EDS analysis			XRD analysis		
		Exp. compositions of phases (at.%)			Lattice parameters (Å)		
		Cu	In	Ni	*a* this work/literature	*B* this work/literature	*C* this work/literature
1	(Cu) ε'(NiIn)	94.23±0.2 0.67±0.1	0.56±0.4 50.60±0.3	5.21±0.6 48.73±0.2	3.5993(1)/3.625[30] 4.5439(7)/4.545[23]		 4.3569(3)/4.353[23]
2	(Cu) ε'(NiIn)	94.53±0.3 1.03±0.5	0.65±0.7 49.87±0.3	4.82±0.1 49.1±0.4	3.5986(3)/3.625[30] 4.5454(5)/4.545[23]		 4.3503(5)/4.353[23]
3	(Cu) ε'(NiIn)	94.21±0.2 0.49±0.4	0.57±0.6 51.43±0.7	5.22±0.3 48.08±0.5	3.5976(4)/3.625[30] 4.5465(1)/4.545[23]		 4.3556(8)/4.353[23]
4	(Cu) ε'(NiIn)	96.2±0.2 0.81±0.4	0.42±0.6 50.21±0.2	3.38±0.5 48.98±0.2	3.5976(2)/3.625[30] 4.5455(2)/4.545[23]		 4.3505(1)/4.353[23]
5	(Cu) ε'(NiIn)	95.1±0.4 0.66±0.2	0.4±0.4 49.65±0.2	4.5±0.2 49.69±0.1	3.5974(4)/3.625[30] 4.5445(5)/4.545[23]		 4.3563(3)/4.353[23]
6	(Cu) ε'(NiIn)	96.08±0.1 0.67±0.4	0.63±0.4 50.31±0.2	3.29±0.4 49.02±0.1	3.5967(7)/3.625[30] 4.5449(2)/4.545[23]		 4.3549(7)/4.353[23]
7	δ(Cu_7In_3) (Cu) ε'(NiIn)	68.98±0.6 95.04±0.1 0.87±0.5	29.81±0.5 0.3±0.2 48.17±0.6	1.21±0.1 4.66±0.6 50.96±0.3	6.7327(1)/6.733[29] 3.6021(2)/3.625[30] 4.5446(1)/4.545[23]	9.1339(1)/9.134[29]	10.0761(8)/10.074[29] 4.3518(7)/4.353[23]
8	δ(Cu_7In_3) (Cu) ε'(NiIn)	70.18±0.7 94.08±0.3 0.13±0.2	29.15±0.1 0.73±0.4 49.03±0.1	0.67±0.3 5.19±0.2 50.84±0.5	6.7337(2)/6.733[29] 3.6009(7)/3.625[30] 4.5443(7)/4.545[23]	9.1343(2)/9.134[29]	10.0765(1)/10.074[29] 4.3529(4)/4.353[23]
9	δ(Cu_7In_3) Ni_2In_3 η(Cu_2In)	68.74±0.2 0.57±0.3 67.32±0.4	29.54±0.5 61.06±0.3 32.15±0.3	1.72±0.4 38.37±0.1 0.53±0.2	6.7378(1)/6.733[29] 4.3857(1)/4.387[23] 4.2987(1)/4.2943[26]	9.1354(1)/9.134[29]	10.0737(7)/10.074[29] 5.2928(9)/5.295[23] 5.2387(2)/5.2328[26]
10	$Cu_{11}In_9$ Ni_3In_7 η′(CuIn)	54.32±0.3 0.32±0.2 62.28±0.3	44.93±0.2 71.42±0.6 37.24±0.2	0.75±0.7 28.26±0.2 0.48±0.7	12.8139(7)/12.814[28] 9.1799(2)/9.18[24] 4.2498(1)/4.250[27]	4.3557(2)/4.3543[28]	7.3523(2)/7.353[28] 4.9633(9)/4.965[27]
11	L $Cu_{11}In_9$ Ni_3In_7	2.43±0.3 56.93±0.2 0.73±0.1	95.81±0.2 43.05±0.2 69.64±0.3	1.76±0.5 0.02±0.3 29.63±0.8	- 12.8187(7)/12.814[28] 9.1803(5)/9.18[24]	4.3576(1)/4.3543[28]	7.3522(1)/7.353[28]
12	L $Cu_{11}In_9$ Ni_3In_7	3.48±0.5 55.54±0.7 1.15±0.3	95.98±0.5 43.56±0.7 70.89±0.1	0.54±0.1 0.90±0.4 27.96±0.2	- 12.8112(4)/12.814[28] 9.1798(4)/9.18[24]	4.3522(5)/4.3543[28]	7.3545(7)/7.353[28]
13	L $Cu_{11}In_9$ Ni_3In_7	2.7±0.6 54.69±0.5 1.66±0.3	96.34±0.1 44.83±0.4 68.13±0.2	0.96±0.7 0.48±0.2 30.21±0.1	- 12.8156(6)/12.814[28] 9.1799(1)/9.18[24]	4.3587(4)/4.3543[28]	7.3521(2)/7.353[28]
14	L $Cu_{11}In_9$ Ni_3In_7	2.68±0.3 54.10±0.4 0.80±0.1	96.23±0.2 45.83±0.3 70.54±0.3	1.09±0.7 0.07±0.5 28.66±0.3	- 12.8144(2)/12.814[28] 9.1801(5)/9.18[24]	4.3527(1)/4.3543[28]	7.3555(7)/7.353[28]
15	(Cu) ε'(NiIn) ζ`($Ni_{13}In_9$)	92.35±0.4 0.18±0.3 0.43±0.3	0.46±0.7 48.94±0.2 40.04±0.1	7.19±0.1 50.88±0.6 59.53±0.3	3.5885(1)/3.625[30] 4.5473(2)/4.545[23] 14.6433(7)/14.646[25]	 8.3273(6)/8.329[25]	 4.3518(9)/4.353[23] 8.9763(1)/8.977[25]
16	δ(Cu_7In_3) (Cu) ε'(NiIn)	69.58±0.2 97.26±0.1 0.77±0.1	30.01±0.1 1.41±0.7 49.74±0.5	0.41±0.2 1.33±0.7 49.49±0.7	6.7343(1)/6.733[29] 3.6018(1)/3.625[30] 4.5433(6)/4.545[23]	9.1365(1)/9.134[29]	10.0712(3)/10.074[29] 4.3518(8)/4.353[23]
17	δ(Cu_7In_3) (Cu) ε'(NiIn)	70.04±0.2 97.12±0.1 0.14±0.3	28.45±0.6 1.23±0.4 49.33±0.2	1.51±0.3 1.65±0.2 50.53±0.3	6.7329(8)/6.733[29] 3.6023(7)/3.625[30] 4.5423(2)/4.545[23]	9.1339(2)/9.134[29]	10.0733(3)/10.074[29] 4.3545(1)/4.353[23]
18	δ(Cu_7In_3) Ni_2In_3 ε'(NiIn)	69.13±0.1 0.17±0.1 0.13±0.5	28.93±0.3 30.25±0.4 51.31±0.5	1.94±0.5 69.58±0.4 48.56±0.4	6.7334(9)/6.733[29] 4.3844(6)/4.387[23] 4.5439(4)/4.545[23]	9.1355(1)/9.134[29]	10.0765(3)/10.074[29] 5.2977(6)/5.295[23] 4.3565(4)/4.353[23]

According to the thermodynamic calculations, (see Fig. 1) samples 1 to 6 belong to the two-phase region (Cu)+ ε'(NiIn). The obtained experimental results for these six alloy samples confirm the existence of this two-phase region. In all cases, the solubility of copper in intermetallic phase ε'(NiIn) was found to be less than 1 at. % and thus it was negligible. Also in the case of the solid solution (Cu), the detected solubility of In was negligible. The other obtained results related to the identified phases were found to be the same as predicted so the existence of all predicted regions was confirmed. Moreover, the subsequent XRD analysis has also confirmed the presence of the same phases as were predicted by thermodynamic calculations and determined by EDS analysis. Figure 2 shows microstructures of the six alloy samples selected out of nineteen studied alloys. Sample 6 belongs to the two-phase region while the rest samples 8, 9, 10, 11 and 12 are from three-phase regions. The phases identified using the results of energy dispersive spectrometry (EDS) are marked on the presented microstructures.

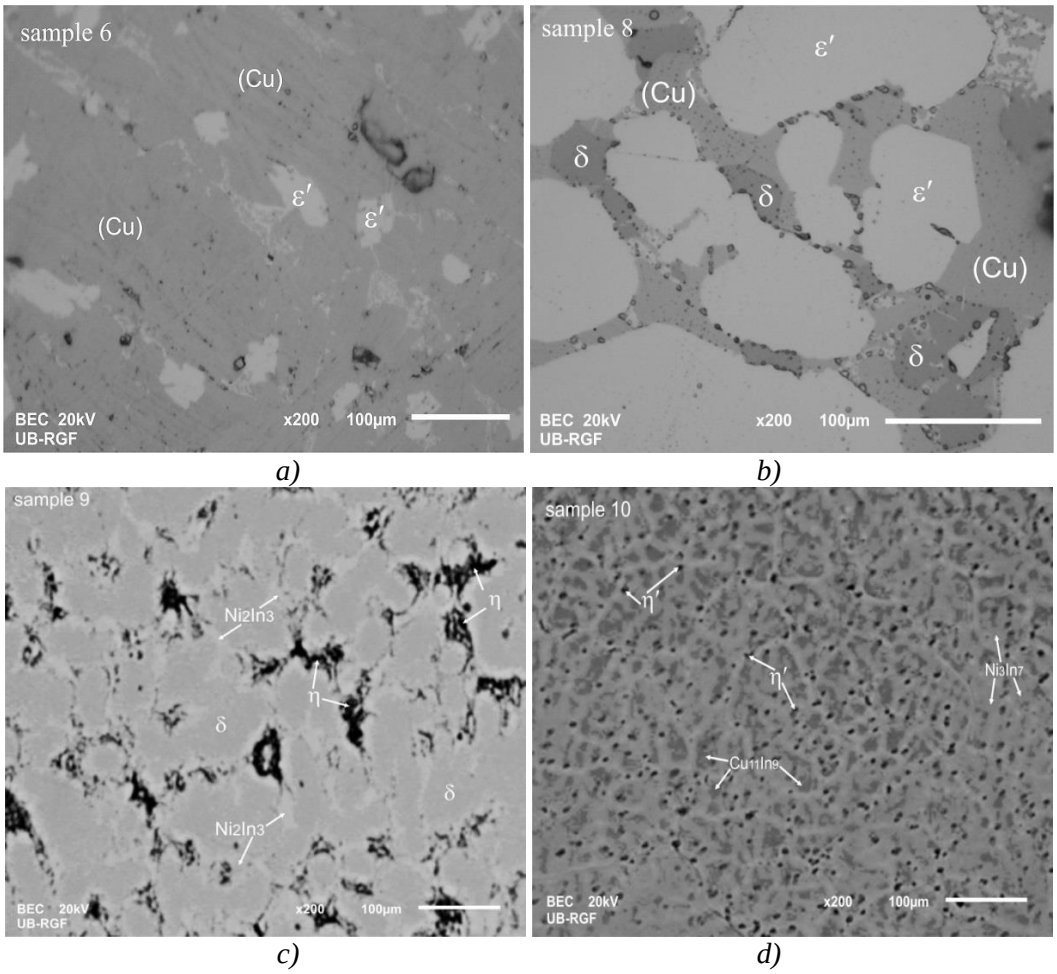

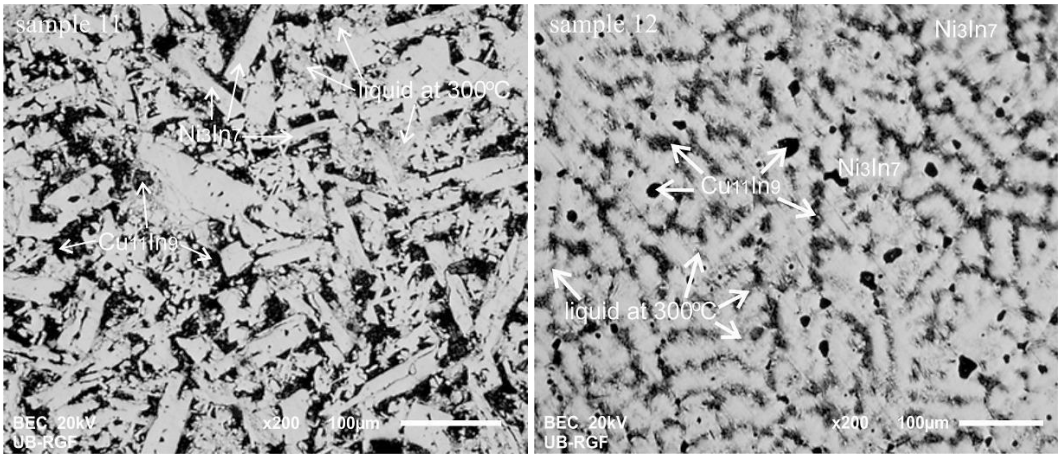

e) *f)*

Fig. 2. Microstructures of the alloys analyzed using SEM-EDS technique: a) sample 6, b) sample 8, c) sample 9, d) sample 10, e) sample 11 and f) sample 12

In microstructure of sample 6, two phases are visible, solid solution (Cu) which is a dominant phase and binary intermetallic compound ε'(NiIn). Three-phase region δ(Cu_7In_3) + (Cu) + ε'(NiIn) is visible at the microstructure of sample 8. The alloy samples 9 and 10 (Fig.2c and Fig.2d) also belong to three-phase regions. As can be seen from Fig.2c the δ phase is the most dominant phase within the microstructure of sample 9 whereas Ni_2In_3 intermetallic compound appears as light phase situated at its grain boundaries. The alloy sample 10 (Fig.2d) seems to have more fine-grained microstructure compared to the rest of the studied alloy samples. In its microstructure (Fig.2d) η′ phase can be observed as a small, black and round phase evenly distributed throughout the microstructure of the alloy. The samples 11 and 12 belong to the three-phase region in which liquid phase L is present (L+Ni_3In_7+$Cu_{11}In_9$). It can be observed in Fig.2e and Fig.2f as the dark phase trapped between intermetallic compounds. The intermetallic compound $Cu_{11}In_9$ appears as the darkest phase in the microstructures of the alloy samples 11 and 12 while the Ni_3In_7 intermetallic compound is the most abundant phase.

Lattice parameters of the detected phases were compared with lattice parameters from literature [23-30]. Two XRD patterns with identified phases, one for the sample 1 and the other for the sample 15 are shown in Figure 3, as an illustration.

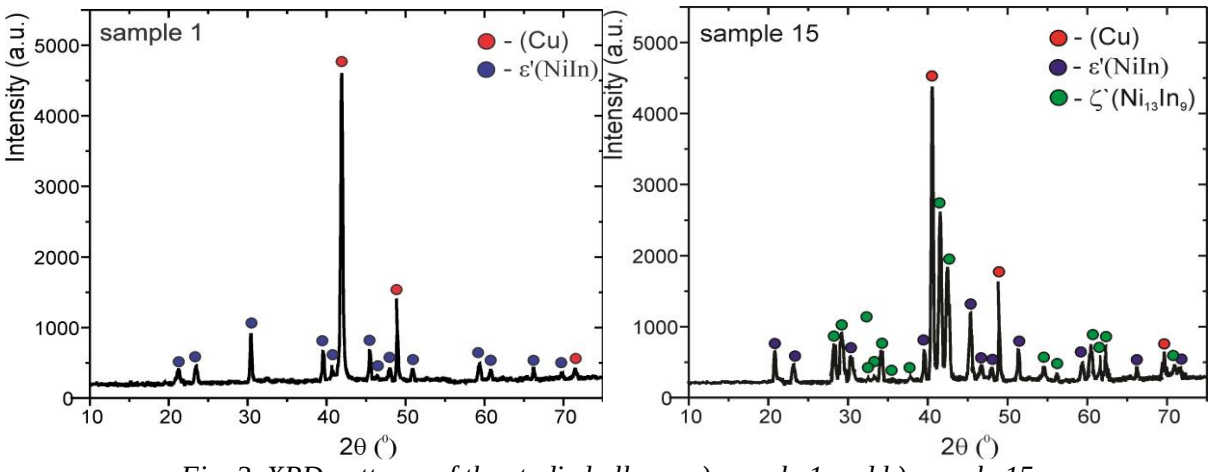

Fig. 3. XRD patterns of the studied alloys: a) sample 1 and b) sample 15

From Table 2 it can be seen that the experimentally determined values of lattice parameters for a solid solution (Cu) slightly vary for different alloy samples between 3.5885(1) Å and 3. 6023(7) Å. This discrepancy can be explained by taking into account high solubility of nickel in solid solution (Cu) e.g. determined value of a lattice parameter for (Cu) phase in sample 15 is shifted towards the lower value and considering that lattice parameter for (Ni) phase are $a=b=c$=3.499 Å [31]. It can be assumed that the obtained results may be related to the solubility of nickel.

4. CONCLUSION

Isothermal section at 300 ºC of the Cu-In-Ni ternary system was investigated using SEM-EDS and XRD analyses and computed using optimized thermodynamic parameters from literature. Compositions of the investigated alloys were along three vertical sections Cu–$In_{0.5}Ni_{0.5}$, In-$Cu_{0.8}Ni_{0.2}$, and x(In) = 0.4 of the studied ternary system. Experimentally investigated microstructures and determined phase compositions of the studied alloy samples equilibrated at 300 °C show close agreement with the results of thermodynamic calculation.

ACKNOWLEDGEMENTS

This work was supported by the Ministry of Education, Science and Technological Development of the Republic of Serbia, under Projects No. ON172037 and TR37020.

5. REFERENCE

[1] Chen J., Wang J., Yan F., Zhang Q and Li, Q. Tribol. Int., 81 (2015) 1–8.,
[2] Carrera A., Cangiano M., Ojeda M. and Ruiz M. Mater. Charact., 101 (2015) 40–48.,
[3] Cui S., Zhang L., Du Y., Zhao D., Xu H., Zhang W. and Liu S., Calphad, 35 (2011) 231–241.,
[4] Xu X., Zhu N., Zheng W., and Xi. Lun, Calphad, 52 (2016) 78–87.,
[5] Semboshi S., Sato S., Iwase A. and Takasugi T., Mater. Charact., 115 (2016) 39–45.,
[6] Lei J., Hui X. Tao Shiping, Rong Z. and Zhenlin L., Rare Metal Mat. Eng., 44(12) (2015) 3050 3054.,
[7] Samal C.P., Parihar J.S. and Chaira D., J. Alloys Comp. 569 (2013) 95–101.,
[8] Masrour R., Hamedoun M., Benyoussef A. and Hlil E.K., J. Magn. Magn. Mater., 363 (2014) 15.,
[9] Badawya W.A., El-Rabiee M., Helal N.H. and Nady H., Electrochim. Acta, 71 (2012) 50-57.,
[10] Calleja P., Esteve J., Cojocaru P., Magagnin L., Valles E. and Gomez E., Electrochim. Acta 62 (2012) 381–389.,
[11] Nagarjuna S., Srinivas M. and Sharma K.K., Acta Mater. 48 (2000) 1807–1813.,
[12] Milosev I. and Metikos-Hukovic M., Electrochim. Acta, 42(10) (1997) 1537-1548.,
[13] B. Li, J. Gu, Q. Wang, C. Ji, Y. Wang, J. Qiang and C. Dong, Mater. Charact., 68 (2012) 94-101.,
[14] C. Ganley Jason, Int. J. Hydrogen Energy, 34(9) (2009) 3604-3611.,
[15] Minić D., Premović M., Ćosović V., Manasijević D., Nedeljković Lj. and Živković D., J. Alloys Comp., 617 (2014) 379–388.,
[16] Premović M., Manasijević D., Minić D. and Živković D., Kovove Mater., 54(1) (2016) 45-53.,
[17] Premović M., Minić D., Manasijević I. and Živković D., Mater. Test.,57(10) (2015) 883-888.,
[18] Minić D., Aljilji A., Kolarević M., Manasijević D. and Živković D., High Temp. Mater. Proc.,30(1-2) (2011) 131–138.,
[19] H.S. Liu, X.J. Liu, Y. Cui, C.P. Wang, I. Ohnuma, R. Kainuma, Z.P. Jin and K. Ishida, J. Phase Equilibria, 23 (5) (2002) 409–415.,
[20] Waldner P. and Ipser H., Z. Metallkd., 93(8) (2002) 825–832.,
[21] S. an Mey, Z. Metallkd. 78 (1987) 502.,
[22] Cao W., Chen S.L., Zhang F., K. Wu, Yang Y., Y.A. Chang, R. Schmid-Fetzer and W.A. Oates, Calphad 33(2) (2009) 328-342.,
[23] Hellner E., Metallkd Z., 41 (1950) 401-406.,
[24] Baranova R.V. and Pinsker Z.G., Kristallografiya, 10(5) (1965) 614-621.,
[25] Ellner M., Bhan S. and Schubert K., J. Less-Common Met. 19 (1969) 245–252.,

[26] Che G. C. and Ellner M., Powder Diffr., 7(2) (1992) 107-108.,
[27] Ramos S. de Debiaggi, Cabeza G.F., Deluque Toro C., Monti A. M., Sommadossi S., and Fernandez Guillermet A., J. Alloys Comp., 509 (2011) 3238-3245.,
[28] Rajasekharan T. and Schubert K., Z. Metallkd., 72 (1981) 275-278.,
[29] Lidin S., Stenberg L., and Elding-Ponten M., J. Alloys Compd, 255 (1997) 221-226.,
[30] Srinavasa Rao S. and Anantharaman T.R., Acta Crystallogr. Sec. A 32 (1963) 262–263.,
[31] Davey W.P., Phys. Rev. 25 (1925) 753–761.